Estimation Method for Mass Transfer Coefficient Distribution using Near-Infrared Spectroscopy

Eshima, Hiroshi
Interdisciplinary Graduate School of Engineering Sciences, Kyushu University

Ikegaya, Naoki
Interdisciplinary Graduate School of Engineering Sciences, Kyushu University

Yasumasu, Takuya
Interdisciplinary Graduate School of Engineering Sciences, Kyushu University

Hagishima, Aya
Interdisciplinary Graduate School of Engineering Sciences, Kyushu University

他

https://doi.org/10.5109/4372278

出版情報：Evergreen. 8 (1), pp.193-197, 2021-03. 九州大学グリーンテクノロジー研究教育センター
バージョン：

Estimation Method for Mass Transfer Coefficient Distribution using Near-Infrared Spectroscopy

Hiroshi Eshima[1], Naoki Ikegaya[1*], Takuya Yasumasu[1], Aya Hagishima[1], Jun Tanimoto[1]

[1] Interdisciplinary Graduate School of Engineering Sciences, Kyushu University

6-1 Kasuga-koen, Kasuga-shi, Fukuoka 816-8580, Japan

*Author to whom correspondence should be addressed:
E-mail: ikegaya.naoki@kyudai.jp

(Received October 12, 2020; Revised March 26, 2021; accepted March 26, 2021).

Abstract: Various experimental studies were conducted to reveal the distribution of the heat and mass transfer coefficients over complex geometries using classical techniques, such as the wet filter paper and salinity methods. However, such methods cannot determine the spatial distribution of the transfer coefficients with high resolution because they are based on area-averaged mass changes during a certain period. Therefore, we propose a new estimation technique for determining the distribution of the transfer coefficients by applying near-infrared (NIR) spectroscopy. In our method, NIR light is incident on a wet filter paper, and the reflection intensity of the paper is measured using a high-response NIR camera. The water mass content of the paper is determined by the reflection intensity based on a calibration equation that establishes the relationship between water mass content and the reflection intensity. The results showed the measurement error was less than 7%. In this paper, we report basic trials to confirm the accuracy and applicability of the technique for a boundary layer over a smooth surface.

Keywords: Heat transfer coefficient; mass transfer coefficient; near-infrared spectroscopy

1. Introduction

Heat and mass transfer coefficients between an urban area and the atmosphere are key factors in determining the heat budget within the urban area. An accurate estimation of the transfer coefficient for complex urban surfaces is essential for better numerical prediction of the momentum and heat budget within urban areas, because most computational fluid dynamics approaches employ interfacial models to express the momentum and mass transport between a surface and the air above due to convection[1-9].

As convective heat loss is usually difficult to estimate, mass transfer coefficients are alternatively determined by assuming similarity between mass and heat transfer. In addition, wind tunnel experiments with various turbulence generators are commonly used[10,11] to reproduce outdoor turbulence structures represented by the Kaimal or Karman spectrum[12,13]. For example, Barlow et al.[14,15] and Pascheke et al.[16] employed a naphthalene sublimation method to determine the mass transfer amount over complex geometries in a series of wind-tunnel experiments. In addition, Narita[17] and Chung et al.[18] reported a spatially averaged transfer coefficient for complex geometries and locations, by using a filter paper method, in which the mass change during the experiment was directly measured by using an electric balance. Furthermore, Hagishima et al.[19] and Ikegaya et al.[20-23] employed a salinity method to accurately determine the mass transfer coefficients for various types of urban geometries in a series of wind-tunnel experiments.

In these methods, however, the mass changes due to exposure of the target to airflow are measured by weighing a specimen or by the change in the salinity. Therefore, these methods can estimate the spatially averaged transfer coefficient. Although Narita[16] employed the filter paper method to determine the spatial distribution of the transfer coefficient, the spatial resolutions of the measurements are not sufficiently high because of the limitations of the measurement techniques. Moreover, the measurement error in weighing the specimen directly affects the estimation accuracy of the transfer coefficient. Although such weighing of the specimen is considerably sensitive to experimental procedures, no feasible alternative is available.

Under these circumstances, Asawa et al.[24,25] proposed a new technique to estimate the mass transfer coefficient by applying near-infrared spectroscopy (NIRS) for full-scale experiments with a three-dimensional laser scanner. In this method, the water content in a target object can be

estimated from the reflection intensity of near-infrared (NIR) light from the object, because NIR light is absorbed by water molecules due to the absorption wavelength of water. However, they concluded that relative errors in the mass estimation by the reflection of NIR light are still large because of the full-scale experiments. Therefore, following this idea, but applying it to small-scale wind-tunnel experiments, we propose an NIRS method by employing an NIR light source and NIR camera, to estimate the water mass content in a specimen. In this paper, we report basic trials to confirm the accuracy and applicability of the proposed NIRS method in determining the spatial distribution of the mass transfer coefficient for boundary layers over smooth surfaces.

2. Method

2.1. Definition of transfer coefficient

The mass transfer coefficient, k [m/s], between a wet surface and the air above is defined by

$$k = \frac{E}{C_s - C_a}, \quad (1)$$

where E [kg/m^{2}s] denotes the evaporation rate per unit area and time, and C_s and C_a [kg/m^3] denote the vapor concentrations on the wet surface and at the reference position, respectively. C_s can be calculated by assuming that the vapor concentrations on the wet surface is saturated at the surface temperature T_s. Because k represents the transport speed of the vapor, the normalized value C_E is defined as

$$C_E = \frac{k}{U_{ref}}, \quad (2)$$

where U_{ref} denotes the reference wind speed [m/s]. C_E is also known as the Stanton number or bulk transfer coefficient.

Temporally averaged E can be determined by the mass change M_{eva} [kg] of the wet surface with an area of A [m^2] during a period T [s] due to evaporation as follows:

$$E = \frac{M_{eva}}{AT}. \quad (3)$$

To determine M_{eva}, a conventional method known as the wet filter paper technique[16,17] can be used to calculate the mass change during period T by measuring the mass before and after the exposure of a specimen to air flows using a high-accuracy electric mass balance. The technique is simple and easy for calculating M_{eva}; however, it requires careful treatment of the specimen of the wet filter paper, to avoid mass change during mass measurement. In addition, a certain amount of mass change through T is required for the accurate measurement of M_{eva}. Because of this limitation, spatial distributions with high resolutions of M_{eva} cannot be determined by this method.

Another method called the salinity method[22] employs salt water as the water source. In this method, the salinity in the water is measured before and after exposure. This enables us to determine the mass change through T with very high accuracy; however, it also requires a large measurement area to maximize the change in salinity.

2.2. NIRS method

We applied NIRS to estimate the mass change—NIRS enables estimation of the mass change without any contact with the specimen. It is known that NIR light with wavelength ranging from 800 to 2500 nm is absorbed by water molecules owing to the several specific absorption wavelengths of water (approximately 1450 nm and 1940nm). When NIR light is irradiated on a wet filter paper, light is repeatedly reflected and refracted on and within the wet filter paper. During this process, light with specific wavelengths is absorbed by the wet filter paper. Consequently, the reflection intensity of the corresponding wavelengths is weak compared with those of other wavelengths. By using these characteristics, we can correlate the reflection intensity and the gravimetric water content (GWC). GWC, denoted as w[-], is defined as

$$w(t) = \frac{M_w(t)}{M_p + M_w(t)}, \quad (4)$$

where M_p [kg] and M_w [kg] indicate the weight of the dried filter paper and the water mass content of the wet filter paper, respectively. M_w is a function of time because of water evaporation; therefore, M_{eva} can be determined by

$$M_{eva} = w(t_b) - w(t_a), \quad (5)$$

where t_b [s] and t_a [s] represent the time before and after an experiment with $T=t_b-t_a$.

The relation between the reflection intensity r and w is determined empirically by calibration experiments, as explained in Section 2.3. The following relationship is obtained for $0.45 < w < 0.55$:

$$w = Ar + B, \quad (6)$$

where A and B are empirical coefficients estimated by the least square method.

Because the reflection and refraction characteristics within the wet filter paper depend on w, the linear relationship of Eq. (2) is applicable only in the specified range of GWC. To determine the reflection rates, an NIR camera is employed, which can provide the reflection intensity of each pixel of an image. Therefore, the empirical coefficients in Eq. (6) are determined for each

measurement point. We require only the camera images of the reflection intensity to determine the water content of the paper; therefore, the proposed NIRS method is a new non-intrusive and spatially-resolved approach to estimate the transfer coefficient.

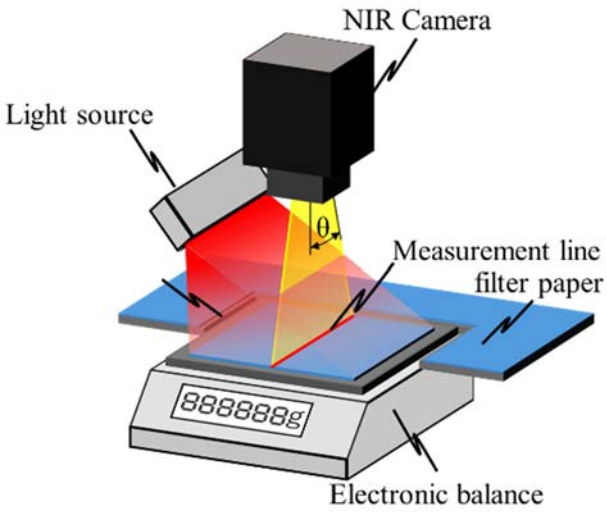

Fig. 1: Schematic of the calibration system of NIRS.

2.3. Calibration

The NIRS method requires a calibration equation to determine the relation between the reflection intensity and water content. Fig. 1 shows a schematic of the calibration experiments. NIR light from an NIR light-emitting diode (KKIMAC, IDBA-C100) was irradiated on a filter paper of size 200 mm × 200 mm placed on an electronic balance (A&D, FZ-500i). The surrounding surfaces of the wet paper was also covered by wet filter paper to avoid a rapid change in the evaporation rate near the edge of the measured paper. The reflected light was captured by an NIR camera (ARTRAY, ARTCAM-L512TNIR), which can record the brightness at 512 points on the measurement line with a brightness resolution of 8 bits. The incident angle θ is defined as the angle between the line through the center of the camera to the center of the paper, and the line through the center of the camera and each measurement point.

In the calibration experiments, the wet filter paper was naturally dried on the electronic balance by NIR light for approximately 2 h. The weight of the paper was measured by the electric balance every 1 s. Simultaneously, the brightness of the image was captured by the NIR camera every 1 s.

Fig. 2 shows an example of the relationship between w and r at the center of the images (θ=0). The line indicates the calibration formula in Eq. (6), determined by the least squares method. As w decreases, r monotonically increases because of the absorption of NIR light by water molecules. The linear relationship is applicable in the range $0.45<w<0.55$. Similar relationships between w and r can be seen in the other measurement positions; however, the values of r strongly depend on θ. This is because of both directional sensitivity of the brightness and the sensitivity of the camera sensor detecting light intensity at each pixel. Therefore, the empirical coefficients A and B are determined for each pixel of an image.

Fig. 3 shows the relative errors between GWC directly measured by the electric balance and the GWC determined by Eq. (4). The horizontal axis in Fig. 3 refers to the number of pixels in the image. As seen from the figure, the relative error fluctuated for every 20 pixels approximately. This could be due to the slightly undulating surface of the wet filter paper. However, the relative errors are less than 7% except for the edges, indicating that the NIRS method can predict GWC with acceptable errors.

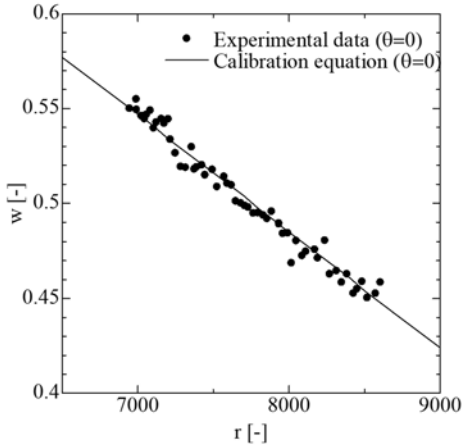

Fig. 2: Relationship between brightness intensity r captured by the NIR camera and gravity weight contents (GWC) w. The linear line represents the calibration equation $w=Ar+B$.

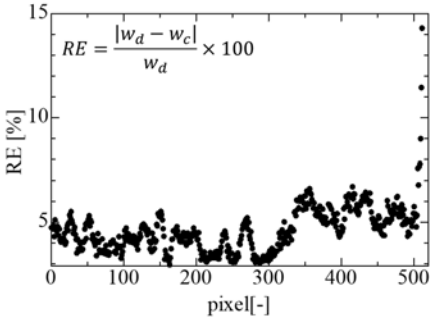

Fig. 3: Relative errors at each pixel. w_d: GWC measured by the electric balance, w_c: GWC determined by Eq. (4), after the calibration experiments.

3. Application to a smooth surface

3.1 Experimental setup

As a simple application of NIRS, we estimated the transfer coefficient distribution on a smooth surface under a turbulent boundary layer. Fig. 4 (a) shows a schematic of the experimental setup. The test section of the open-circuit wind tunnel was 0.5 m wide, 0.5 m high, and 7.36 m long. A smooth boundary layer was generated by a plate

installed within the wind tunnel. The plate was located at the spanwise center and 130 mm away from the bottom of the wind tunnel to ensure that the approach flow to the plate was vertically and horizontally uniform. On the plate, a wet filter paper of size 200 mm × 200 mm was attached to estimate the transfer coefficient distribution in the streamwise direction. The light source device, NIR camera, and thermography camera (ARGO, Xi400) were installed above the plate to supply continuous NIR light to the wet filter paper and to capture r for the distribution of both w and T_s (surface temperature). T_s is also obtained using thermistors (Techno Seven, DS101) inserted in the paper at three points (Fig. 4 (b)). The temperature distribution measured by the thermography camera was corrected based on the mean temperature of the three thermistors.

The reference wind velocity U_{ref}, dew point temperature of the air T_{dew}, and the reference position temperature T_{air} were measured using a pitot static tube (LK-1S, OKANO WORKS, LTD.), a dew point hygrometer (Dew Star S-1, SHINYEI Technology Co., Ltd.), and thermistors, respectively.

The wet filter paper was exposed to the wind with U_{ref}~2 m/s for a period of T (s). While exposing the paper to the wind, r and T_s were continuously measured every 30 s by the NIR camera and thermography camera. We determined the distribution of C_E by taking temporally averaged values for all quantities in Eq. (1), for every 64 pixels.

To confirm the accuracy of the NIRS method, the area-averaged C_E is estimated using the wet filter paper method as well.

3.2 C_E distribution on a smooth surface

Fig. 5 shows the distribution of C_E on the smooth surface measured with the NIRS and the filter paper methods. The horizontal axis indicates the streamwise distance x from the upstream edge of the smooth boundary layer. The results of the NIRS method at each streamwise position represent the area-averaged C_E for areas divided into eight parts of the entire wet filter paper, with error bars indicating the standard deviation of C_E in the area. In addition, the gray-hatched area represents the relative errors in Fig. 3. Moreover, the entire area-averaged C_E is also shown by the dotted line. The figure shows that C_E obtained by the NIRS method drops sharply near the upstream edge and gradually decreases with the streamwise distance, although the standard deviation is large, because of the position of the camera and the filter paper. This is a plausible tendency because the scalar boundary layer develops rapidly near the upstream edge and gradually deepens in the streamwise direction. In addition, all the area-averaged C_E values obtained with NIRS and the filter paper methods agree well. These results indicate that the NIRS method is applicable for estimating C_E for a boundary layer over a simple smooth surface.

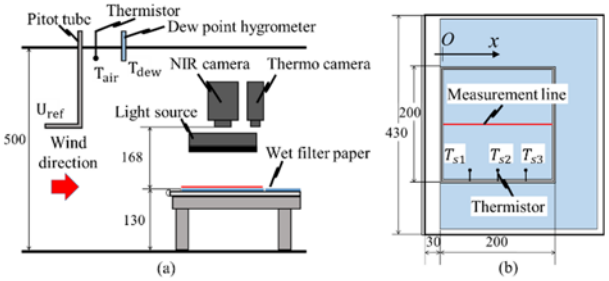

Fig. 4: Schematic of the wind-tunnel experiment for estimating the transfer coefficient distribution on the wall of a boundary layer over a smooth surface. (a) Side view of the wind tunnel, and (b) plane view of the wet filter paper and measurement line.

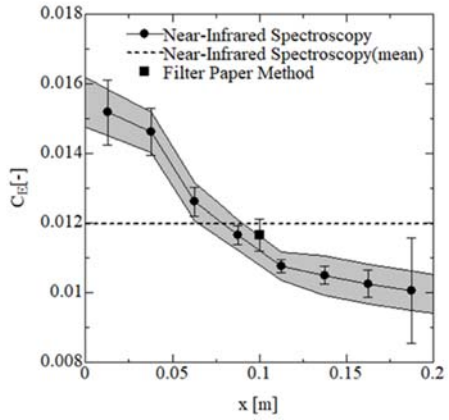

Fig. 5: Streamwise distribution of C_E. Filled circles and squares represent the bulk coefficients obtained using the NIRS method and the filter paper method, respectively. The filter paper method only determined the spatial averaged value of C_E.

4. Conclusions

We proposed a new measurement method using NIRS to reveal the distribution of the transfer coefficient over smooth surfaces. First, we confirmed that intensity of NIR has a linear relationship with the gravimetric water content in the calibration experiment. Based on this fact, the calibration coefficients were determined for the NIRS method. Second, we measured the distribution of C_E on the bottom wall of a boundary layer over a smooth surface. The C_E values obtained by NIRS and the conventional wet filter paper method were consistent.

Based on these fundamental results, we conclude that the proposed NIRS method can be widely used as a non-intrusive method for determining C_E.

References

1) V.B.L. Boppana, Z.T. Xie, and I.P. Castro, "Large-eddy simulation of dispersion from surface sources in arrays of obstacles," *Boundary-Layer Meteorol.*, **135** (*3*) 433–454 (2010). doi:10.1007/s10546-010-9489-9.
2) X.M. Cai, J.F. Barlow, and S.E. Belcher, "Dispersion and transfer of passive scalars in and above street canyons-large-eddy simulations," *Atmos. Environ.*, **42**

(*23*) 5885–5895 (2008). doi:10.1016/j.atmosenv.2008.03.040.
3) S. Branford, O. Coceal, T.G. Thomas, and S.E. Belcher, "Dispersion of a point-source release of a passive scalar through an urban-like array for different wind directions," *Boundary-Layer Meteorol.*, **139** (*3*) 367–394 (2011). doi:10.1007/s10546-011-9589-1.
4) V.B.L. Boppana, Z.T. Xie, and I.P. Castro, "Thermal stratification effects on flow over a generic urban canopy," *Boundary-Layer Meteorol.*, **153** (*1*) 141–162 (2014). doi:10.1007/s10546-014-9935-1.
5) V.B.L. Boppana, Z.T. Xie, and I.P. Castro, "Large-eddy simulation of heat transfer from a single cube mounted on a very rough wall," *Boundary-Layer Meteorol.*, **147** (*3*) 347–368 (2013). doi:10.1007/s10546-012-9793-7.
6) Y. Ikeda, A. Hagishima, N. Ikegaya, J. Tanimoto, and A.A. Razak, "Estimation of wind speed in urban pedestrian spaces on the basis of large-eddy simulation," *J. Environ. Eng.*, **80** (*709*) 259–267 (2015). doi:10.3130/aije.80.259.
7) N. Ikegaya, A. Hagishima, and J. Tanimoto, "Large-eddy simulation on scalar transfer phenomena between urban surface and atmosphere," J. Environ. Eng. (Transactions AIJ), 76 (668) 943–951 (2011). doi:10.3130/aije.76.943.
8) N. Mohd, M.M. Kamra, M. Sueyoshi, and C. Hu, "Lattice boltzmann method for free surface impacting on vertical cylinder: a comparison with experimental data," *Evergreen*, **4** (*2–3*) 28–37 (2017). doi:10.5109/1929662.
9) C. Li and K. Ito, "Performance evaluation of wind decontamination system by computational fluid dynamics," *Evergreen*, **1** (*2*) 12–17 (2014). doi:10.5109/1495158.
10) J. Counehan, "Wind tunnel determination of the roughness length as a function of the fetch and the roughness density of three-dimensional roughness elements," *Atmos. Environ.*, **5** (*8*) 637–642 (1971). doi:10.1016/0004-6981(71)90120-X.
11) N.A. Rahmat, A. Hagishima, N. Ikegaya, and J. Tanimoto, "Experimental study on effect of spires on the lateral nonuniformity of mean flow in a wind tunnel," *Evergreen*, **5** (*1*) 1–15 (2018). doi:10.5109/1929670.
12) A.M.M. Ismaiel, and S. Yoshida, "Study of turbulence intensity effect on the fatigue lifetime of wind turbines," *Evergreen*, **5** (*1*) 25–32 (2018). doi:10.5109/1929727.
13) A.M. Halawa, B. Elhadidi, and S. Yoshida, "POD & MLSM Application on DU96-W180 wind Turbine airfoil", *Evergreen* **5** (1) 36–43 (2017).
14) J.F. Barlow, I.N. Harman, and S.E. Belcher, "Scalar fluxes from urban street canyons. part i: laboratory simulation," *Boundary-Layer Meteorol.*, **113** (*3*) 369–385 (2004). doi:10.1023/B:BOUN.0000045525.70731.ff.
15) I.N. Harman, J.F. Barlow, and S.E. Belcher, "Scalar fluxes from urban street canyons. part ii: model," *Boundary-Layer Meteorol.*, **113** (*3*) 387–409 (2004). doi:10.1023/B:BOUN.0000045526.07270.a3.
16) F. Pascheke, J.F. Barlow, and A. Robins, "Wind-tunnel modelling of dispersion from a scalar area source in urban-like roughness," *Boundary-Layer Meteorol.*, **126** (*1*) 103–124 (2008). doi:10.1007/s10546-007-9222-5.
17) K. Narita, "Experimental study of the transfer velocity for urban surfaces with a water evaporation method," *Boundary-Layer Meteorol.*, **122** (*2*) 293–320 (2007). doi:10.1007/s10546-006-9116-y.
18) J. Chung, A. Hagishima, N. Ikegaya, and J. Tanimoto, "Wind-tunnel study of scalar transfer phenomena for surfaces of block arrays and smooth walls with dry patches," *Boundary-Layer Meteorol.*, **157** (*2*) 219–236 (2015). doi:10.1007/s10546-015-0063-3.
19) A. Hagishima, J. Tanimoto, S. Suenaga, N. Ikegaya, K. Maeda, and K. Narita, "Wind tunnel experiment on bulk scalar coefficient of urban-like roughness," *J. Environ. Eng.* **73**, 1225–1231 (2008). doi:10.3130/aije.73.1225.
20) N. Ikegaya, A. Hagishima, J. Tanimoto, and Y. Tanaka, "A study on the similarity of the momentum and scalar roughness lengths over urban-like roughness," J. Environ. Eng. (Transactions AIJ), 77 (681) 917–923 (2012). doi:10.3130/aije.77.917.
21) N. Ikegaya, A. Hagishima, J. Tanimoto, and Y. Tanaka, "A study on the similarity of the momentum and scalar roughness lengths over urban-like roughness," *J. Environ. Eng.* **80** (*711*) 451–459 (2015). doi:10.3130/aije.80.451.
22) N. Ikegaya, A. Hagishima, J. Tanimoto, Y. Tanaka, and K. Narita, "Effects on bulk scalar coefficient of wind angle, development of scalar boundary layer, and flow field near roughness," J. Environ. Eng. (Transactions AIJ), 76 (659) 67–73 (2011). doi:10.3130/aije.76.67.
23) N. Ikegaya, A. Hagishima, J. Tanimoto, S. Suenaga, K. Maeda, and K. Narita, "Measurement of Mass Transfer Coefficients Using Salinity Method", The Society of Heating, Air-Conditioning Sanitary Engineers of Japan, **34** (*147*) 57–60 (2009). doi:10.18948/shase.34.147_57.
24) T. Asawa and T. Kiyono, "Visualization of convective heat transfer coefficient on building external surfaces using a 3D laser scanner and the filter paper evaporation method Part 4: Improving accuracy and precision in spatio-temporal distributions," Architectural Institute of Japan, Summaries of technical papers of annual meeting, D-1, p.869 (2018). https://ci.nii.ac.jp/naid/200000433963/en/.
25) T. Kiyono, T. Asawa, and H. Oshio, "Laser-scanning-based method for estimating the distribution of the cnovective -heat transfer coefficient on full-scale building walls", *Boundary-Layer Meteorol*. (2020). https://doi.org/10.1007/s10546-020-00578-x